World Academy of Science, Engineering and Technology
International Journal of Physical and Mathematical Sciences
Vol:8, No:7, 2014

Using Printing Method and Post Heat Treatment to Fabricate CIS Absorber Layer

Mao-An Chen, Chien-Chen Diao, Chia-Cheng Huang, Chin-Guo Kuo, Cheng-Fu Yang, Yen-Lin Chen

Open Science Index, Physical and Mathematical Sciences Vol:8, No:7, 2014 publications.waset.org/9998743/pdf

***Abstract*—**In this study, the Mo-electrode thin films were deposited using two-stepped process and the high purity copper indium selenide-based powder ($CuInSe_2$, CIS) was fabricated by using hydrothermal process by Nanowin Technology Co. Ltd. Because the CIS powder was aggregated into microscale particles, the CIS power was ground into nano-scale particles. 6 wt% CIS particles were mixed and dispersed into isopropyl alcohol (IPA). A new non-vacuum thin-film deposition process, spray coating method (SPM), was investigated to deposit the high-densified CIS absorber layers. 0.1 ml CIS solution was sprayed on the 20 mm×10 mm Mo/glass substrates and then the $CuInSe_2$ thin films were annealed in a selenization furnace using N_2 as atmosphere. The annealing temperature and time were set at 550^{o}C and 5 min, and 0.0g~0.6g extra Se content was added in the furnace. The influences of extra Se content on the densification, crystallization, resistivity (ρ), hall mobility (μ), and carrier concentration of the CIS absorber layers were well investigated in this study.

***Keywords*—**$CuInSe_2$, isopropyl alcohol, spray coating method, annealing, selenization process.

I. Introduction

SCIENTIFIC interest in renewable energy resources, in particular, solar energy technologies that employ efficient and robust photovoltaic cells have been high-lighted. $Cu(In,Ga)Se_2$ (CIGS) [1] and $CuInSe_2$ (CIS) [2] are two of the most promising. Used as a light absorbing material, CIGS is of high interest to the areas of solar cell research and production. The CIGS and CIS systems are known to have some advantages such as non-toxicity, long time stability, and high conversion efficiency. Several methods have been reported to fabricate CIGS and CIS absorber thin films and sputtering and co-evaporation are two of the most popular methods. R. Wuerz et al. used the co-evaporation process to fabricate the highly efficient CIS absorber layers on different substrates [3] and Hsu et al. used the sputtering and selenization processes to deposit the CIGS absorber layers [4]. Traditional vacuum methods are too complicated and difficult because those methods require a large number of expensive equipments, when the number of process parameters increases.

The spray pyrolysis method (SPM) is a very important deposition method to fabricate thin films because it has the merits of relatively simple, non-vacuum, and inexpensive for large-area coating [5]. In this study, the CIS precursor was synthesized by using the hydrothermal process by Nanowin Technology Co. Ltd. Even having nano-scale particle sizes, the formed CIS powder was aggregated in the microscale, for that we needed to grind the CIS powder into nano-scale particle sizes. A SPM was used to investigate the CIS absorber layers with high densification structure. However, only few efforts had been made to systematically investigate the effects of thermal-treated parameters in a selenization furnace on the physical and electrical properties of the CIS absorber layers. We would investigate the effects of extra Se content on the physical and electrical properties of the CIS absorber layers.

II. Experimental Procedure

Back electrode layer functions as a barrier that hinders the diffusion of impurities from the substrates into the absorber layers. In this study, the corning eagle XG glass (thickness was 0.7 mm) with the size 20 mm×10 mm was used as substrates to deposit the bi-layer-structured Mo electrode at room temperature in pure argon. After the surfaces of the glass substrates were cleaned then they put into the sputter. At first, the chamber was pumped to 8×10^{-6} Torr, the first layer of Mo was deposited at the deposition parameters of power of 50W, working pressure of 10 m Torr, and Ar flow rate of 70 sccm for 6.5 min; The second layer of Mo was deposited at the deposition parameters of power of 50W, working pressure of 5 m Torr, and Ar flow rate of 20 sccm for 29 min, respectively. The first layer had a thickness of ~ 116 nm and the second layer had a thickness of ~ 327 nm. The high purity copper indium selenide-based (CIS) powder was synthesized and formed using hydrothermal process by Nanowin Technology Co. Ltd. Because the CIS precursor was aggregated into micro-scale particles, as Fig. 1 (a) shows, the milling ball with the average diameter of 0.2 mm was used to grind them into nano-scale particles. The morphology of the ground CIS powders were observed using transmission scanning electron microscope (TEM). As Fig. 1 (b) shows, the ground powers were really showed the nano-scale particles. After finding the optimum grinding time and KD1 content, the 6 wt% CIS particle was dispersed into isopropyl alcohol (IPA) to get the solution for SPM to prepare the CIS absorber layers. The organic/CIS

Mao-An Che and Yen-Lin Chen are with the Department of Chemical and Materials Engineering, National University of Kaohsiung, Taiwan, Kaohsiung, 81148, R.O.C. (e-mail: top19901212@hotmail.com, cpr4511@hotmail.com).

Cheng-Fu Yang is with the Department of Chemical and Materials Engineering, National University of Kaohsiung, Taiwan, Kaohsiung, 81148, R.O.C. (corresponding author to provide phone: 886-7-5919283; fax: 886-7-5919277; e-mail: cfyang@nuk.edu.tw).

Chien-Chen Diao is with the Department of Electronic Engineering, Kao Yuan University, Kaohsiung 82151, Taiwan, R.O.C. (e-mail: t10025@cc.kyu.edu.tw).

Chia-Cheng Huang is with the Environmental Protection Bureau Kaohsiung City Government, Kaohsiung, Taiwan, R.O.C. (e-mail: jon19830102@outlook.com).

Chin-Guo Kuo is with the Department of Industrial Education, National Taiwan Normal University, Taipei 10610, Taiwan, R.O.C. (e-mail: chinguo7@yahoo.com.tw).

Open Science Index, Physical and Mathematical Sciences Vol:8, No:7, 2014 publications.waset.org/9998743/pdf

composite films were formed by SCM on Mo/glass by using the same volume of CIS/IPA solution, and then the organic/CIS composite films were annealed by using the rapid temperature annealing (RTA) process in selenization furnace (the chamber size is 5cm x 5cm x 4cm) to remove the used organic and crystallize the CIS absorber layers. 550°C and 5 min were used as the annealing temperature and time, and 0.0 g~0.6 g extra Se content was put in the furnace during the annealing process. After annealing process, the crystalline structure was examined by using XRD pattern and the surface morphology and cross section observations of the CIS absorber layers were examined by using the FESEM, respectively. The electrical resistivity and the Hall-effect coefficients were measured using a Bio-Rad Hall set-up.

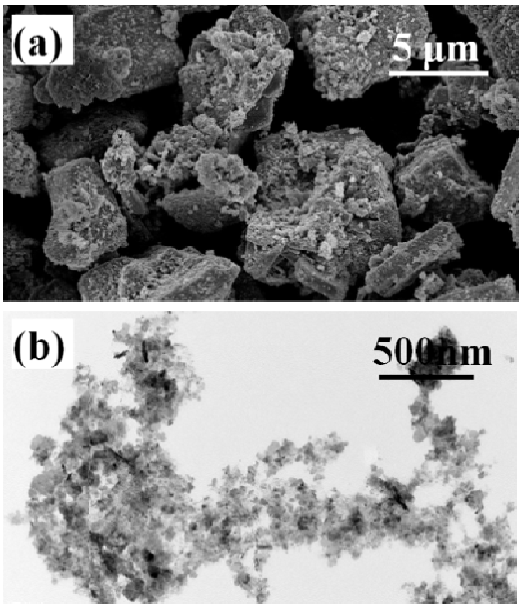


Fig. 1 CIS precursors observed in (a) aggregated state (b) after dispersing

III. Results and Discussion

In this study, we used 550°C as the temperature to develop the characteristics of the CIS absorber layers under different extra Se content used during the selenization process. The XRD patterns of the CIS absorber layers as a function of extra Se content were investigated, and the results are shown in Fig. 2. Fig. 2 shows that only the CIS phase was observed and no secondary phases were observed even the extra Se content was 0.6 g. As extra Se content was 0.0 g, 0.1 g, 0.2 g, and 0.6 g, the (112) peak revealed in Fig. 2 was situated at 2θ = 26.68°, 26.62°, 26.58°, and 26.58°, respectively. This result suggests that the lattice constant of the CIS absorber layers increased with increasing extra Se content. The FWHM value of the (112) peak of the CIS absorber layers was 0.424, 0.456, 0.531, and 0.587 as extra Se content was 0.0 g, 0.1 g, 0.2 g, and 0.6 g, respectively. Too much extra Se content is not necessary because the crystallinity of the CIS absorber layers will be inhibited. Fig. 2 also shows that the relative diffraction intensity of (112) peak critically decreased and the relative diffraction intensity of (110) peak critically increased as extra Se content increased from 0.0 g to 0.6 g. This is because as extra Se content is used, the more Se will vaporize and diffuse into CIS absorber layers during the selenization process to inhibit the grain growth and distort the lattice, then the FWHM value increases, the relative diffraction intensity of (112) peak decreases, and the relative diffraction intensity of (110) peak increases.

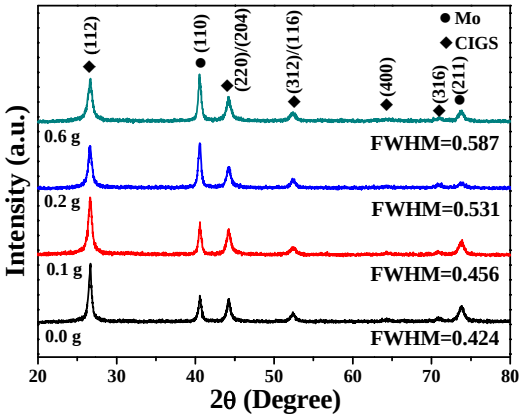


Fig. 2 XRD patterns of the CIS absorber layers as a function of extra Se content

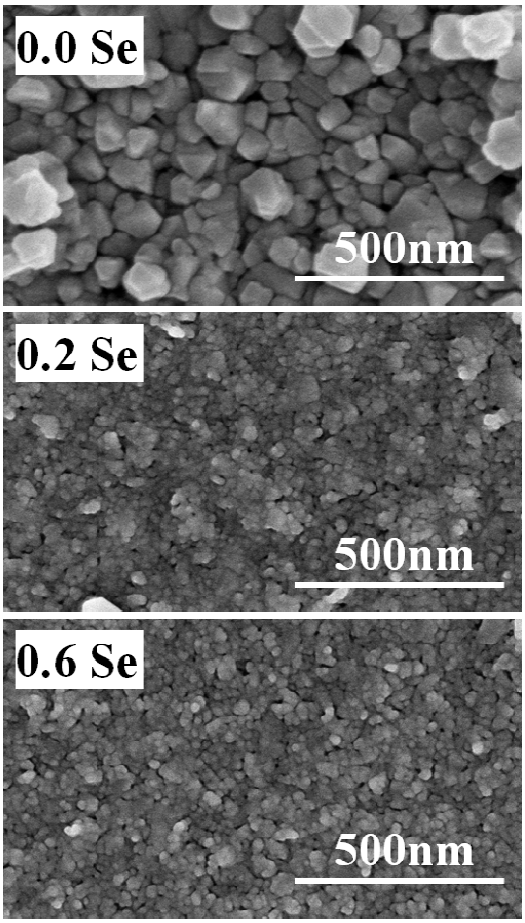


Fig. 3 Surface morphologies of the CIS absorber layers as a function of extra Se content

Open Science Index, Physical and Mathematical Sciences Vol:8, No:7, 2014 publications.waset.org/9998743/pdf

Fig. 3 shows the surface morphologies of the CIS absorber layers as a function of extra Se content, the selenization temperature was 550°C, and the results in Fig. 3 have large difference as the different extra Se content was added. As no extra Se was added in the furnace (0.0 g), the grain growth and roughness surface were really observed. The surface morphologies shown in Fig. 3 apparently reveal that the grain sizes of the CIS absorber layers apparently decreased with increasing extra Se content. As extra Se content was used equal and more than 0.2 g, even the densified and flat surfaces were observed, the grain growth in the CIS absorber layers were inhibited. Those results suggest that as selenized process is used, the extra Se content is important to control the characteristics of the CIS absorber layers. The CIS absorber layers selenized at less extra Se content have the better crystalline structure but will cause more pores.

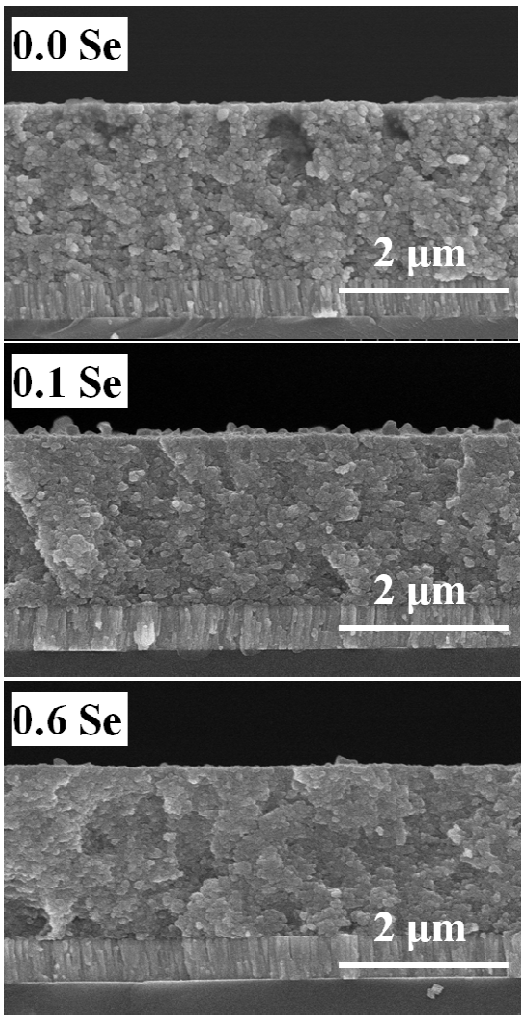


Fig. 4 Cross section observations of the CIS absorber layers as a function of extra Se content

Also, the cross morphologies of the CIS absorber layers as a function of extra Se content were also observed, and the results were compared in Fig. 4. The thicknesses of the CIS absorption layers were around 1905 ± 50 nm. As no extra Se was put in the furnace (0.0 g), even the large grains grow is observed on the surface, a densified structure was observed in the cross section. However, the results in Fig. 4 show prove that the densified and crystallized CIS absorber layers can be obtained by using the SPM and RTA in a selenization furnace, and the extra Se content is a more important effect to influence the CIS absorbers' characteristics.

Fig. 5 shows the dependence of electrical properties of the CIS absorber layers as a function of extra Se content in the selenized process. The carrier concentration decreased from 1.15 $\times 10^{22}$ cm^{-3} to 8.30 $\times 10^{18}$ cm^{-3}, the carrier mobility increased from 1.75 cm^2/V-s to 1487 cm^2/V-s, and the resistivity increased from 2.75 $\times 10^{-4}$ Ω-cm to 5.06 $\times 10^{-4}$ Ω-cm as extra Se content increased from 0.0 g to 0.6 g, respectively. From the SEM surface and cross morphologies shown in Figs. 2 and 3, the crystallinity can decrease because too much extra Se content used in the selenization process will inhibit the crystallization of the CIS absorber layers. The carrier mobility will decrease because the increase of defects will inhibit the carrier movement.

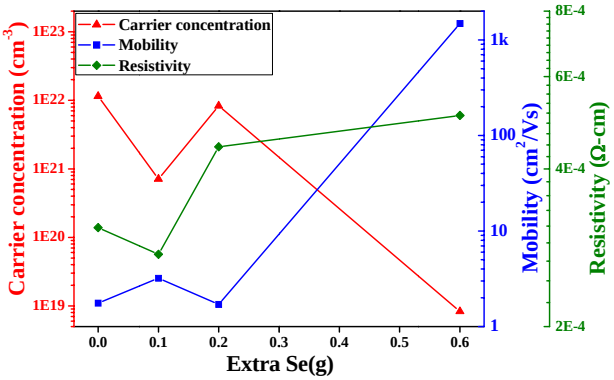


Fig. 5 Resistivity (ρ), Hall mobility (μ), and carrier concentration (n) of the CIS absorber layers as a function of extra Se content

IV. Conclusion

As extra Se content was 0.0 g, 0.1 g, 0.2 g, and 0.6 g, the (112) peak was situated at 2θ = 26.68°, 26.62°, 26.58°, and 26.58°; The FWHM value of the (112) peak of the CIS absorber layers was 0.424, 0.456, 0.531, and 0.587; The relative diffraction intensity of (112) peak decreased and the relative diffraction intensity of (110) peak increased, respectively. The thicknesses of the CIS absorption layers were around 1905 ± 50 nm. As extra Se content was 0.0 g, 0.1 g, 0.2 g, and 0.6 g, the carrier concentration decreased from 1.15 $\times 10^{22}$ cm^{-3} to 8.30 $\times 10^{18}$ cm^{-3}, the carrier mobility increased from 1.75 cm^2/V-s to 1487 cm^2/V-s, and the resistivity increased from 2.75 $\times 10^{-4}$ Ω-cm to 5.06 $\times 10^{-4}$ Ω-cm, respectively.

Acknowledgment

The authors acknowledge financial supports of Nanowin Technology Co. Ltd., NSC 101-2221-E-244 -006, NSC 102-2622-E-390 -002-CC3, and NSC 102-2221-E-390-027.

REFERENCES

[1] M. Li, M. Zheng, T. Zhou, C. Li, L. Ma, and W. Shen, "Fabrication and characterization of ordered $CuIn_{(1-x)}Ga_xSe_2$ nanopore films via template-based electrodeposition," Nanoscale Res Lett, vol. 7, paper ID 675, 2012.

[2] A. Cho, S. Ahn, J.H. Yun, J. Gwak, S.K. Ahn, K. Shin, H. Song, and K.H. Yoon, "Non-vacuum processed $CuInSe_2$ thin films fabricated with a hybrid ink,", Solar Energy Mater. & Solar Cells, vol. 109, pp. 17–25, 2013.

[3] M. Powalla, G. Voorwinden, D. Hariskos, P. Jackson, R. Kniese, "Highly efficient CIS solar cells and modules made by the co-evaporation process," Thin Solid Films, vol. 517, no. 7, pp. 2111–2114, 2009.

[4] C.Y. Hsu, P.C. Huang, Y.Y Chen, D.C. Wen, "Fabrication of a $Cu(InGa)Se_2$ Thin Film Photovoltaic Absorber by Rapid Thermal Annealing of CuGa/In Precursors Coated with a Se Layer," Intern. J. Photoenergy, vol. 2013, paper ID 132105, 2013.

[5] C.C. Wu, C.F. Yang, "Investigate the Properties of Nanostructured Li-doped NiO Films Using the Modified Spray Pyrolysis Method," Nanoscale Res Lett, vol. 8, paper ID 33, 2013.

Open Science Index, Physical and Mathematical Sciences Vol:8, No:7, 2014 publications.waset.org/9998743/pdf